Spectrochimica Acta Part A: Molecular and Biomolecular Spectroscopy 116 (2013) 160–164

Contents lists available at ScienceDirect

Spectrochimica Acta Part A: Molecular and Biomolecular Spectroscopy

journal homepage: www.elsevier.com/locate/saa

The molecular structure of the borate mineral inderite $Mg(H_4B_3O_7)(OH)\cdot 5H_2O$ – A vibrational spectroscopic study

Ray L. Frost [a,*], Andrés López [a], Yunfei Xi [a], Rosa Malena Fernandes Lima [b], Ricardo Scholz [c], Amanda Granja [c]

[a] School of Chemistry, Physics and Mechanical Engineering, Science and Engineering Faculty, Queensland University of Technology, GPO Box 2434, Brisbane, Queensland 4001, Australia
[b] Mining Engineering Department, School of Mines, Federal University of Ouro Preto, Campus Morro do Cruzeiro, Ouro Preto, MG 35400-00, Brazil
[c] Geology Department, School of Mines, Federal University of Ouro Preto, Campus Morro do Cruzeiro, Ouro Preto, MG 35400-00, Brazil

HIGHLIGHTS

- Inderite $Mg(H_4B_3O_7)(OH)\cdot 5H_2O$ is a hydrated hydroxy borate mineral of magnesium.
- We have studied inderite by elcctron probe, thermogravimetry and vibrational spectroscopy.
- The mineral decomposes at 137.5 °C.
- Raman bands are observed at 3052, 3233, 3330, 3392 attributed to water stretching vibrations.
- Vibrational spectroscopy enables the assessment of its molecular structure.

GRAPHICAL ABSTRACT

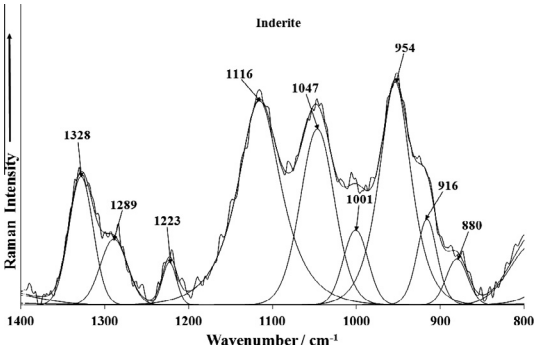

ARTICLE INFO

Article history:
Received 13 March 2013
Received in revised form 23 June 2013
Accepted 28 June 2013
Available online 6 July 2013

Keywords:
Inderite
Borate
Raman spectroscopy
Infrared
Pinnoite

ABSTRACT

We have undertaken a study of the mineral inderite $Mg(H_4B_3O_7)(OH)\cdot 5H_2O$ a hydrated hydroxy borate mineral of magnesium using scanning electron microscopy, thermogravimetry and vibrational spectroscopic techniques. The structure consists of $[B_3O_3(OH)_5]^{2-}$ soroborate groups and $Mg(OH)_2(H_2O)_4$ octahedra interconnected into discrete molecules by the sharing of two OH groups. Thermogravimetry shows a mass loss of 47.2% at 137.5 °C, proving the mineral is thermally unstable. Raman bands at 954, 1047 and 1116 cm^{-1} are assigned to the trigonal symmetric stretching mode. The two bands at 880 and 916 cm^{-1} are attributed to the symmetric stretching mode of the tetrahedral boron. Both the Raman and infrared spectra of inderite show complexity. Raman bands are observed at 3052, 3233, 3330, 3392 attributed to water stretching vibrations and 3459 cm^{-1} with sharper bands at 3459, 3530 and 3562 cm^{-1} assigned to OH stretching vibrations. Vibrational spectroscopy is used to assess the molecular structure of inderite.

Introduction

Boron compounds are used in different ways by the industry, including the production of borosilicate glass, enamels, leather, detergents, cosmetics, insulation and textile-grade fibers, fire retardants, fertilizers, insecticides, disinfectants, drugs, alternative energy source and nuclear technology [1–4]. In recent years, the interest for magnesium borates is increasing. Such compounds shows potential applications as catalysts for the conversion of hydrocarbons, luminescent materials, cathode ray tube screens, X-ray screens, electro conductive treating agent, reinforcing agent for plastics and for the production of magnesium diboride [5,6]. Approximately 60% of world boron ores are located in Turkey, mainly in Anatolia. Boron is founds in borates of metals, especially of calcium and sodium [7].

The mineral inderite $Mg(H_4B_3O_7)(OH)\cdot 5H_2O$ [8] is a hydrated hydroxy borate mineral of magnesium [9,10] and was first

* Corresponding author. Tel.: +61 7 3138 2407; fax: +61 7 3138 1804.
E-mail address: r.frost@qut.edu.au (R.L. Frost).

1386-1425/$ - see front matter © 2013 Elsevier B.V. All rights reserved.
http://dx.doi.org/10.1016/j.saa.2013.06.108

described from Inder deposit, Kazakhstan [11]. The mineral was also described from a number of localities, including Inyo Co., California, USA [12] and Kirka borate deposit, Turkey [13].

The mineral is monoclinic [10,14] with Point Group: 2/*m*. The cell data is space group: *P*21/*a* with $a = 12.0350(9)$, $b = 13.1145(13)$, $c = 6.8221(3)$ and $\beta = 104.552(8)$ and $Z = 4$.

The structure consists of $[B_3O_3(OH)_5]^{2-}$ soroborate groups and $Mg(OH)_2(H_2O)_4$ octahedra interconnected into discrete molecules by the sharing of two OH groups [10]. The fifth H_2O molecule is placed in the spaces between these molecular units. The structure is held together by hydrogen bonds. Inderite is a member of the homonymous group that also includes inderborite – $CaMg(H_3B_3O_7)\cdot 8H_2O$, inyoite – $Ca(H_4B_3O_7)(OH)\cdot 4H_2O$, kurnakovite – $Mg(H_4B_3O_7)(OH)\cdot 5H_2O$, meyerhofferite – $Ca(H_4B_3O_7)\cdot 4H_2O$ and solongoite – $Ca_2(H_4B_3O_7)(OH)Cl$.

To the best knowledge of the authors, data about vibrational spectroscopic characterization of inderite are restricted to the database of the University of Arizona (rruff.info); however no interpretation is given. In recent years, the application of spectroscopic techniques to understand the structure of borates has been increasing. Vibrational spectroscopy has been applied to borate glasses [15]. The number of vibrational spectroscopic studies of borate minerals is quite few [16,17]. The number of Raman studies of borate minerals is also very limited [18]. There have been a number of infrared studies of some natural borates [19,20].

In this work, a sample of the mineral inderite from the Inyo Co., located in the Death Valley, California, USA, was selected for analysis. Studies include chemistry via Scanning Electron microscope (SEM) in the EDS mode, spectroscopic characterization of the structure with infrared and Raman spectroscopy. Thermogravimetric study was carried out to determine the thermal stability of the mineral.

Experimental

Samples description and preparation

The inderite sample studied in this work was obtained from the collection of the Geology Department of the Federal University of Ouro Preto, Minas Gerais, Brazil, with sample code SAB-072. The sample is from the type locality for the mineral, the Inyo Co., located in the Death Valley, California, USA.

The borate mineral deposit in the Death Valley is related to the Miocene-Pliocene Furnace Creek Formation, deposited in marginal lacustrine and lacustrine environments in an extensional setting. The bedded borate facies comprises bodies of borate, mainly colemanite. Other minerals are ulexite, probertite, gypsum and anhydrite [21]. The sample was gently crushed and the associated minerals were removed under a stereomicroscope Leica MZ4. Scanning electron microscopy (SEM) and backscattering images (BSI) were obtained to ensure the purity of the selected fragment. Qualitative chemical analysis was applied to support the mineral characterization.

Scanning electron microscopy (SEM)

Experiments and analyses involving electron microscopy were performed in the Center of Microscopy of the Universidade Federal de Minas Gerais, Belo Horizonte, Minas Gerais, Brazil (http://www.microscopia.ufmg.br).

Inderite crystals were coated with a 5 nm layer of evaporated carbon. Secondary Electron and Backscattering Electron images were obtained using a JEOL JSM-6360LV equipment. Qualitative and semi-quantitative chemical analyses in the EDS mode were performed with a ThermoNORAN spectrometer model Quest and was applied to support the mineral characterization.

Thermogravimetric analysis – TG/DTG

TG/DTG analysis of the inderite were obtained by using TA Instruments Inc. Q50 high-resolution TGA operating at a 10 °C/min ramp with data sample interval of 0.50 s/pt from room temperature to 1000 °C in a high-purity flowing nitrogen atmosphere (100 cm^3/min). A total mass of 23.29 mg of finely ground samples were heated in an open platinum crucible.

Raman microprobe spectroscopy

Crystals of inderite were placed on a polished metal surface on the stage of an Olympus BHSM microscope, which is equipped with 10×, 20×, and 50× objectives. The microscope is part of a Renishaw 1000 Raman microscope system, which also includes a monochromator, a filter system and a CCD detector (1024 pixels). The Raman spectra were excited by a Spectra-Physics model 127 He–Ne laser producing highly polarized light at 633 nm and collected at a nominal resolution of 2 cm^{-1} and a precision of ±1 cm^{-1} in the range between 200 and 4000 cm^{-1}. Repeated acquisitions on the crystals using the highest magnification (50×) were accumulated to improve the signal to noise ratio of the spectra. Raman Spectra were calibrated using the 520.5 cm^{-1} line of a silicon wafer. The Raman spectrum of at least 10 crystals was collected to ensure the consistency of the spectra.

An image of the inderite crystals measured is shown in the supplementary information as Fig. S1. Clearly the crystals of inderite are readily observed, making the Raman spectroscopic measurements readily obtainable.

Infrared spectroscopy

Infrared spectra were obtained using a Nicolet Nexus 870 FTIR spectrometer with a smart endurance single bounce diamond ATR cell. Spectra over the 4000–525 cm^{-1} range were obtained by the co-addition of 128 scans with a resolution of 4 cm^{-1} and a mirror velocity of 0.6329 cm/s. Spectra were co-added to improve the signal to noise ratio. The infrared spectra are given in the Supplementary information.

Spectral manipulation such as baseline correction/adjustment and smoothing were performed using the Spectracalc software package GRAMS (Galactic Industries Corporation, NH, USA). Band component analysis was undertaken using the Jandel 'Peakfit' software package that enabled the type of fitting function to be selected and allows specific parameters to be fixed or varied accordingly. Band fitting was done using a Lorentzian–Gaussian cross-product function with the minimum number of component bands used for the fitting process. The Gaussian–Lorentzian ratio was maintained at values greater than 0.7 and fitting was undertaken until reproducible results were obtained with squared correlations of r^2 greater than 0.995.

Results and discussion

Chemical characterization

The SEM image of inderite sample studied in this work is shown in Fig. 1. The image shows a fragment of a single crystal up to 1.5 mm in length. The selected fragment has no zonation or contaminant phases. Qualitative chemical analysis shows a homogeneous phase, composed by Mg and minor amounts of Ca (Fig. 2). The presence of C in EDS spectra is due to carbon coating.

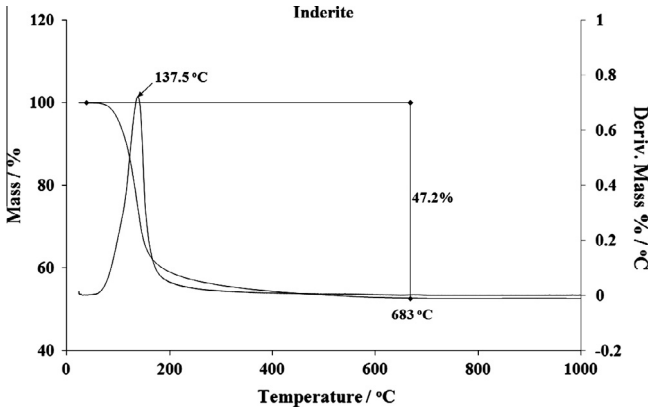

Fig. 1. TG graphic of inderite from 25 to 1000 °C.

The pattern for the thermogravimetric analysis is presented in Fig. 1. The TG curve shows a total mass loss of around 47.20% on heating to 1000 °C. This result is in agreement with the theoretical composition of the mineral. A large mass loss was observed at 137.5 °C, attributed to the loss of water and some hydroxyl units. Some previous studies on inderite have been undertaken [5] and have shown that the mechanism of dehydration is due to random nucleation.

Vibrational spectroscopy

The Raman spectrum of inderite over the 100–4000 cm^{-1} spectral range is shown in Fig. 2(a). This spectrum shows the position and relative intensity of the bands over the full wavenumber range. It is apparent that there are large parts of the spectrum where no intensity is found and therefore, the spectrum is subdivided into sections based upon the type of vibration being studied. The Raman spectrum shows intensity in the hydroxyl stretching region. The infrared spectrum of inderite over the 500–4000 cm^{-1} spectral range is displayed in Fig. 2(b). This figure shows the position and relative intensity of the infrared bands. Again, there are parts of the spectrum where no intensity is observed and thus, the spectrum is subdivided into sections based upon the type of vibration being observed.

As Ross rightly points out the spectra of borate minerals depends heavily on the possible anions in the mineral [22]. The coordination polyhedron around the boron atom will be either a triangle or a tetrahedron. In the case of inderite, the structure consists of linked triangles and tetrahedra. Thus, for inderite the vibrational spectra of both structural units will be observed. The spectra of inderite are complex especially in the infrared spectrum. This is caused by the observation of bands due to four different coordination polyhedra namely BO_3^{3-}, $B(OH)_3$, BO_4^{5-}, and $B(OH)_4^-$.

The Raman spectrum of inderite displays intense Raman bands at 954, 1047 and 1116 cm^{-1} with shoulders at 916 and 1001 cm^{-1}. These bands are assigned to the trigonal symmetric stretching mode. The two bands at 880 and 916 cm^{-1} are attributed to the symmetric stretching mode of the tetrahedral boron. A series of bands are found between 1200 and 1500 cm^{-1}. Raman bands are observed at 1223, 1289 and 1328 cm^{-1}. According to Ross [22] (page 220 of this reference), bands between 1300 and 1500 cm^{-1} are due to the antisymmetric stretching modes of trigonal boron. This is perhaps confirmed by the intensity of the infrared bands in the 1300 to 1500 cm^{-1} region. Infrared bands (Fig. 3(b)) are observed at 1347, 1389, 1414 and 1455 cm^{-1}. The Raman bands at 1213, 1245 and 1281 cm^{-1} are assigned to OH in-plane bending [22]. Infrared bands are found at 1217, 1262 and 1292 cm^{-1} and may be attributed to this vibrational mode. A series of infrared bands are observed at 982, 1013, 1046 and 1093 cm^{-1}. These bands

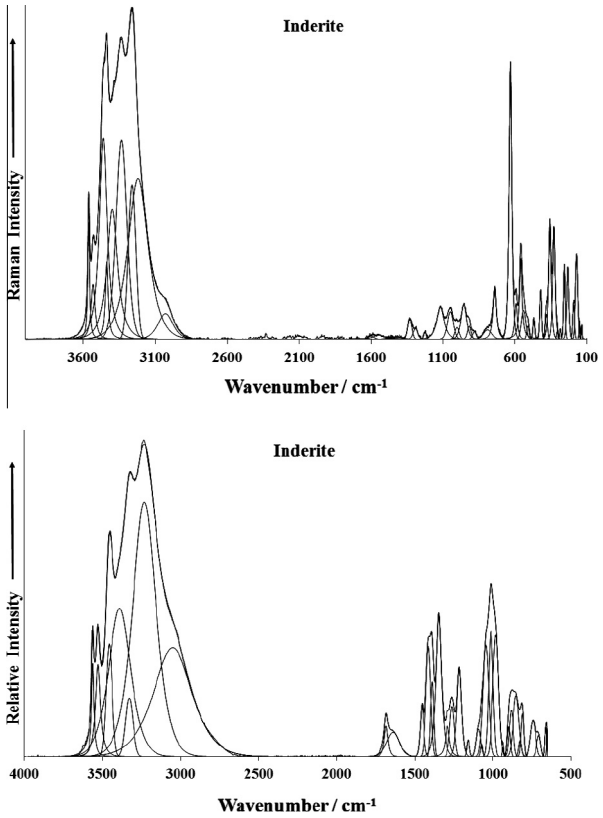

Fig. 2. (a) Raman spectrum of inderite over the 100–4000 cm^{-1} spectral range and (b) infrared spectrum of inderite over the 500–4000 cm^{-1} spectral range.

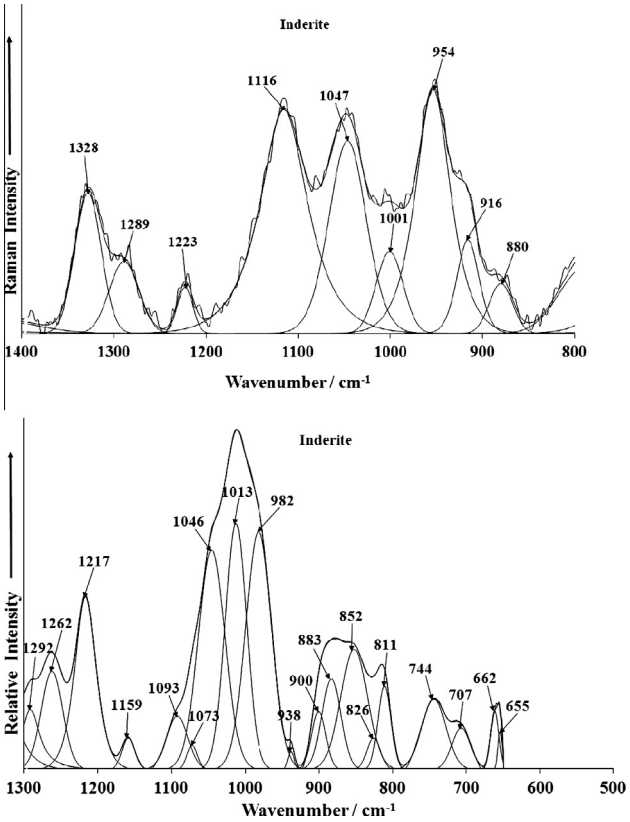

Fig. 3. (a) Raman spectrum of inderite over the 800–1400 cm^{-1} spectral range and (b) infrared spectrum of inderite over the 500–1300 cm^{-1} spectral range.

may be attributed to the symmetric stretching modes of tetrahedral boron.

The Raman spectrum of inderite in the 300–800 cm^{-1} region is illustrated in Fig. 4a and the Raman spectrum in the 100–300 cm^{-1} spectral region is shown in Fig. 4b. The Raman spectrum is dominated by an extremely intense sharp band at 630 cm^{-1} with bands of lower intensity at 558 and 592 cm^{-1}. These bands are attributed to the bending modes of trigonal and tetrahedral boron. The band is not observed in the infrared spectrum, where some low intensity bands are found at 570, 580, 602 and 616 cm^{-1}, which may be assigned to this vibrational mode.

A series of Raman bands are observed at 739 and 788 cm^{-1}. These bands may be assigned to the out-of-plane BOH bending modes. The intensity of these bands is significantly higher in the infrared spectrum (Fig. 3(b)), which is expected. Infrared bands are found at 655, 662, 707, 744 and 766 cm^{-1}. The infrared bands at 811, 826, 852 and 883 cm^{-1} may be assigned to the symmetrical stretching of tetrahedral boron. There have been some studies of the infrared spectra of hydrated borates [20,23]24. In this work, it was concluded that that borate minerals could not be identified by their infrared spectra. The Raman spectrum of inderite in the 100–300 cm^{-1} region is illustrated in Fig. 6(b). Raman bands are observed at 171, 192, 232, 256 cm^{-1} with less intense bands at 135, 151 and 284 cm^{-1}. These bands are simply described as lattice modes.

The Raman and infrared spectra of inderite over the 2600–3800 cm^{-1} spectral range is displayed in Fig. 5. Raman bands are observed at 3052, 3233, 3330, 3392 and 3459 cm^{-1} with sharper bands at 3459, 3530 and 3562 cm^{-1}. The first set of five bands is attributed to water stretching vibrations. The latter three bands are assigned to OH stretching vibrations. The observation of multiple bands fits well with the structure of inderite. The structure consists of $[B_3O_3(OH)_5]^{2-}$ soroborate groups and $Mg(OH)_2(H_2O)_4$ octahedra interconnected into discrete molecules by the sharing of two OH groups. The fifth H_2O molecule is placed in the spaces between these molecular units. The Raman spectrum shows that there are non-equivalent water molecules in the inderite structure. There are different structural units in the structure of inderite. Thus, there are two different types of hydroxyl units and this results in multiple bands attributed to the OH units at 3435, 3459, 3530 and 3560 cm^{-1}.

In some ways the infrared spectrum resembles the Raman spectrum in profile. Intense infrared bands are observed at 3052, 3233, 3330 and 3392 cm^{-1} and are assigned to water stretching vibrations. The infrared bands at 3459, 3530 and 3562 cm^{-1} are attributed to the stretching vibrations of the OH units associated

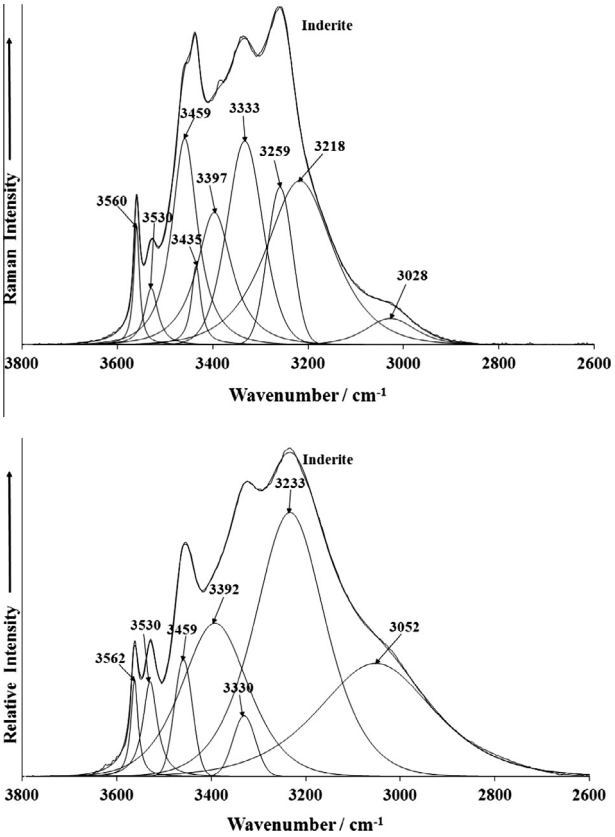

Fig. 5. (a) Raman spectrum of inderite over the 2600–4000 cm^{-1} spectral range and (b) infrared spectrum of inderite over the 2600–4000 cm^{-1} spectral range.

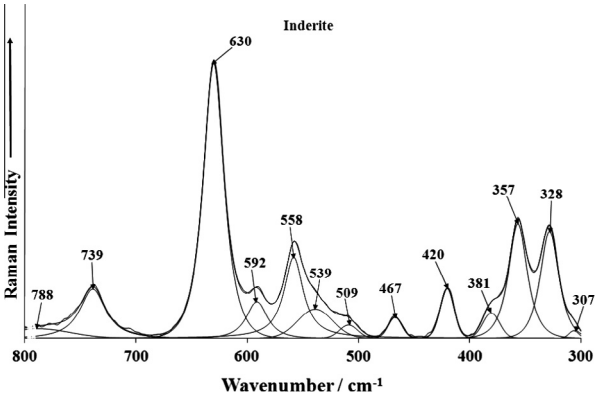

Fig. 4a. Raman spectrum of inderite over the 300–800 cm^{-1} spectral range.

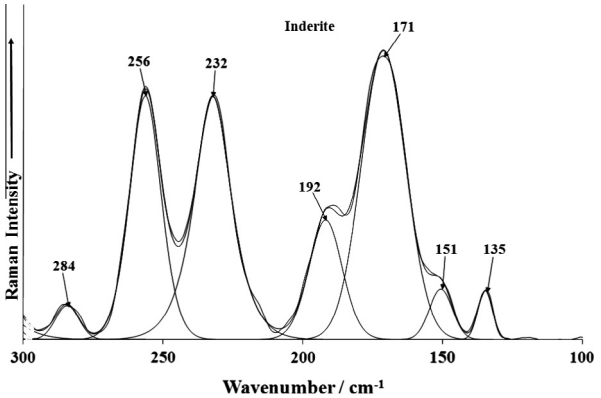

Fig. 4b. Raman spectrum of inderite over the 100–300 cm^{-1} spectral range.

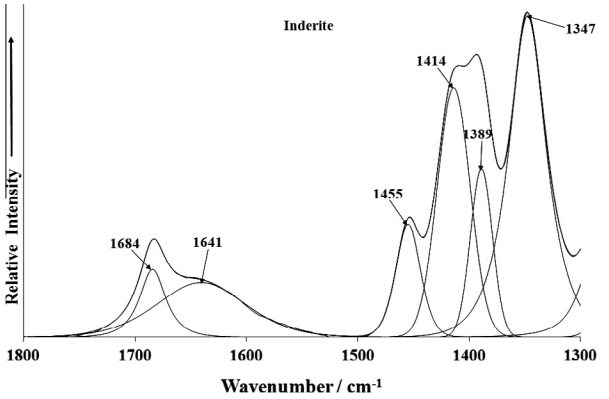

Fig. 6. Infrared spectrum of inderite in the 1300–1800 cm^{-1} spectral range.

with the $[B_3O_3(OH)_5]^{2-}$ soroborate groups and $Mg(OH)_2(H_2O)_4$ units.

The infrared spectrum of inderite in the 1300–1800 cm^{-1} spectral range is illustrated in Fig. 6. In this figure two infrared bands are observed at 1641 and 1684 cm^{-1}, attributed to water bending modes. The position of the infrared bands both in the hydroxyl stretching region and in the water bending region support the concept of strong hydrogen bonding in the structure of inderite. It is reasonable that the water bending modes are not observed in the Raman spectrum. This is because the Raman scattering of water is very low.

Conclusions

The combined chemical characterization of inderite via SEM, EDS and TG shows a pure phase with limited cationic substitution of Mg by Ca. Thermal analysis of inderite shows a large mass loss at 137.48 °C and is thermally unstable.

The structure of inderite consists of $[B_3O_3(OH)_5]^{2-}$ soroborate groups and $Mg(OH)_2(H_2O)_4$ octahedra interconnected into discrete molecules by the sharing of two OH groups and is held together by hydrogen bonds.

Aspects of the structure of inderite may be demonstrated by vibrational spectroscopy. The spectra of borate minerals depend heavily on the possible anions in the mineral. In the case of inderite, the structure consists of linked triangles and tetrahedra. Thus, for inderite the vibrational spectra of both structural units will be observed. The spectra of inderite are complex especially in the infrared spectrum. This is caused by the observation of bands due to four different coordination polyhedra namely BO_3^{3-}, $B(OH)_3$, BO_4^{5-}, and $B(OH)_4^-$.

Acknowledgements

The financial and infra-structure support of the Discipline of Nanotechnology and Molecular Science, Science and Engineering Faculty of the Queensland University of Technology, is gratefully acknowledged. The Australian Research Council (ARC) is thanked for funding the instrumentation. The authors would like to acknowledge the Center of Microscopy at the Universidade Federal de Minas Gerais (http://www.microscopia.ufmg.br) for providing the equipment and technical support for experiments involving electron microscopy. R. Scholz thanks to CNPq – Conselho Nacional de Desenvolvimento Científico e Tecnológico (Grant No. 306287/2012-9). A. Granja offers thanks to FAPEMIG – Fundação de Amparo à Pesquisa do Estado de Minas Gerais.

Appendix A. Supplementary material

Supplementary data associated with this article can be found, in the online version, at http://dx.doi.org/10.1016/j.saa.2013.06.108.

References

[1] K. Othmer, Encyclopedia of Chemical Technology, John Wiley, New York, 1978.
[2] G. Gündüz, A. Usanmaz, J. Nucl. Mater. 140 (1986) 44–55.
[3] M. Özdemir, I. Kipçak, Min. Eng. 23 (2010) 685–690.
[4] F. Demir, G. Budak, R. Sahin, A. Karabulut, M. Oltulu, A. Un, Ann. Nucl. Eng. 38 (2011) 1274–1278.
[5] A.K. Figen, M.S. Yilmaz, S. Piskin, Mater. Char. 61 (2010) 640–647.
[6] E.M. Elssfah, A. Elsanousi, J. Zhang, H.S. Song, C. Tang, Mater. Lett. 61 (2007) 4358–4361.
[7] M. Alkan, M. Dogan, Chem. Eng. Proc. 43 (2004) 867–872.
[8] C. Frondel, V. Morgan, J.L.T. Waugh, Am. Mineral. 41 (1956) 927–928.
[9] A.M. Boldyreva, Mem. Soc. Russe Min. 66 (1937) 651–672.
[10] E. Corazza, Acta Cryst. B32 (1976) 1329–1333.
[11] M.N. Godlevsky, Zap. Vser. Min. Ob. 66 (1937) 315–344.
[12] R.C. Erd, J.F. McAllister, G.D. Eberlein, Am. Mineral. 64 (1979) 369–375.
[13] H. Cahit, R.N. Alonso, Turk. J. Earth Sci. 9 (2000) 1–27.
[14] I.M. Rumanova, A. Ashirov, Krist. 8 (1963) 517–532.
[15] I. Ardelean, S. Cora, J. Optoelect. Adv. Mater. 12 (2010) 239–243.
[16] M. Mir, J. Janczak, Y.P. Mascarenhas, J. Appl. Cryst. 39 (2006) 42–45.
[17] I. Mitov, Z. Cherkezova-Zheleva, V. Mitrov, J. Balkan Trib. Ass. 4 (1998) 191–200.
[18] R.L. Frost, J. Raman Spectrosc. 42 (2011) 540–543.
[19] A. Vasko, I. Srb, Czech. J. Phys. 17 (1967) 1110–1123.
[20] C.E. Weir, J. Res. Nat. Bur. Standards A70 (1966) 153–164.
[21] L.H. Tanner, Sed. Geol. 148 (2002) 259–273.
[22] V.C. Farmer, Mineralogical Society Monograph 4: The Infrared Spectra of Minerals, London, 1974.
[23] E.V. Vlasova, M.G. Valyashko, Zh. Neorgan. Khim. 11 (1966) 1539–1547.